Microchimica Acta (2022) 189: 75
https://doi.org/10.1007/s00604-021-05089-1

ORIGINAL PAPER

T7 Endonuclease I-mediated voltammetric detection of *KRAS* mutation coupled with horseradish peroxidase for signal amplification

Pinky Chowdhury[1] · Byung Seok Cha[1] · Seokjoon Kim[1] · Eun Sung Lee[1] · Taehwi Yoon[1] · Jisu Woo[1] · Ki Soo Park[1]

Received: 31 August 2021 / Accepted: 1 November 2021 / Published online: 27 January 2022

Abstract

Rapid and selective sensing of *KRAS* gene mutation which plays a crucial role in the development of colorectal, pancreatic, and lung cancers is of great significance in the early diagnosis of cancers. In the current study, we developed a simple electrochemical biosensor by differential pulse voltammetry technique for the specific detection of *KRAS* mutation that uses the mismatch-specific cleavage activity of T7-Endonuclease I (T7EI) coupled with horseradish peroxidase (HRP) to catalyze the oxidation of 3,3′,5,5′-tetramethylbenzidine (TMB) substrate in the presence of hydrogen peroxide (H_2O_2). In addition, we synthesized the nanocomposite composed of multi-walled carbon nanotube/chitosan-ionic liquid/gold nanoparticles (MWCNT/Chit-IL/AuNPs) on screen-printed carbon electrode surface to increase the electrode surface area and electrochemical signal. In principle, T7E1 enzyme recognized and cleaved the mismatched site formed by the presence of *KRAS* gene mutation, removing 5′-biotin of capture probes and subsequently reducing the differential pulse voltammetry signal compared to wild-type *KRAS* gene. With this proposed strategy, a limit of detection of 11.89 fM was achieved with a broad linear relationship from 100 fM to 1 μM and discriminated 0.1% of mutant genes from the wild-type target genes. This confirms that the developed biosensor is a potential platform for the detection of mutations in early disease diagnosis.

Keywords *KRAS* G12D mutation · T7-Endonuclease I (T7EI) · Screen-printed carbon electrode · Nanocomposite · Differential pulse voltammetry · Electrochemical biosensor

Introduction

The *KRAS* (Kirsten Ras Sarcoma) gene, which is also known as a proto-oncogene, is one of the human *RAS* gene family that encodes a small GTPase transductor protein called KRAS [1]. Among the three human *RAS* genes (*KRAS*, *NRAS*, and *HRAS*), *KRAS* is the most frequently mutated *RAS* isoform that can lead to the occurrence of various cancers such as pancreatic adenocarcinomas, colorectal cancers (CRCs), and lung adenocarcinomas [2–4]. *KRAS* mutations, which often occur in codon 12 and 13 of exon 2, are present in 35–40% of CRC cases and manifest as an early phenomenon in CRC [5–8]. Thus, KRAS mutations are an attractive therapeutic target for several cancer diseases that can be used to monitor the patient's drug response. Therefore, there is a high demand for specific and quantitative detection strategies for KRAS mutations that will help with prompt initiation of primary treatment.

Currently, different methods have been reported for detection of *KRAS* mutations, most of which rely on gel electrophoresis [9], real-time quantitative polymerase chain reactions [10], pyrosequencing [11], fluorescence spectrometry [12], surface plasmon resonance [13], and electrochemiluminescence [14]. Although these techniques have high sensitivity to *KRAS* mutations, they require relatively expensive instrument and skilled personnel to perform the experiments. In recent years, electrochemical biosensors have received the special attention because of their portability, simplicity, fast response, high sensitivity, and low sample volume. Various electrochemical mutation detection assays, which rely on hybridization, ligation, and nucleotide extension, have been developed to improve the detection sensitivity for low amount of target DNA. These assays are often coupled with signal amplification techniques, such as exonuclease III-aided target recycling [15], rolling circle amplification

✉ Ki Soo Park
akdong486@konkuk.ac.kr; kskonkuk@gmail.com

[1] Department of Biological Engineering, College of Engineering, Konkuk University, Seoul, Republic of Korea

[16], nicking enzyme signal amplification [17], strand-displacement amplification [18], DNA replication [19], enzyme capped gold nanoparticle conjugates [20], single base extension reaction [21], and loop-mediated isothermal amplification [22]. However, these assays can generate high false positive signals and, therefore, have unsatisfactory discrimination power. Aside from improving detection sensitivity, more attention should be paid to enhance the specificity for cancer-related mutations.

In this work, we developed a simple electrochemical strategy by differential pulse voltammetry that relies on the mismatch-specific cleavage activity of the T7 Endonuclease I (T7EI) for the detection of cancer-related mutations. As a model target, *KRAS* c.35G > A (p. G12D) was selected, and the capability of T7EI to recognize and cleave non-perfectly matched DNA was systematically investigated. For improving electrochemical signaling, we prepared nanocomposites composed of amine-functionalized multi-wall carbon nanotube (MWCNT), ionic liquid (IL), chitosan (Chit), and gold nanoparticles (AuNPs) to modify the electrode surface [23]. In addition, horseradish peroxidase-catalyzed reactions were utilized to amplify electrochemical signals.

Experimental section

Materials and reagents

Gold (III) chloride hydrate ($HAuCl_4$, 99.9%), potassium hexacyanoferrate (III), potassium hexacyanoferrate (II), tris(2-carboxyethyl) phosphine, 3,3′,5,5′-tetramethylbenzidine dihydrochloride (TMB), 6-mercaptohexanol (MCH), streptavidin-peroxidase (SA-HRP) polymer, and fetal bovine serum (FBS) were purchased from Sigma-Aldrich, USA. Tetrabutylammonium hydrogen sulfate (Ionic liquid, IL) was purchased from Daejung Chemicals & Metals Co. Limited, Korea. Amine-functionalized Multi-Walled Carbon Nanotube (MWCNT) was synthesized by Adnano Technologies Pvt. Ltd, India. Dulbecco's modified Eagle medium (DMEM) and Roswell Park Memorial Institute (RPMI) 1640 medium were purchased from HyClone (Logan, UT, USA). nPfu-Forte DNA polymerase and T7 endonuclease I (T7EI) were obtained from Enzynomics Co (Daejeon, Korea). All oligonucleotides were synthesized by Integrated DNA Technologies, Inc. USA, and their sequence information is listed in Online Resource 1. Stock solutions of oligonucleotides were prepared in diethylpyrocarbonate (DEPC)-treated water and stored at − 20° C until use. All other chemicals were of analytical-grade purity and used without further purification. All the electrochemical measurements were performed by an Autolab potentiostat/galvanostat, PGSTAT 204 (Metrohm Autolab, The Netherlands) supported by a frequency response analyzer for impedance spectroscopy. Screen-printed carbon electrodes (DRP-C11L) with a diameter of 4 mm and comprising silver pseudo-reference, carbon working, and carbon counter electrodes were obtained from Metrohm DropSens (Asturias, Spain).

Preparation of MWCNT/Chit-IL/AuNP composite

For the preparation of MWCNT/Chit-IL, 5 mg of chitosan was first dissolved in a 1% acetic acid solution and adjusted to pH 5 by 1 N NaOH, to which 2 mg of amine-functionalized MWCNT and 120 µl of 0.1 M IL were then added. The solution was sonicated for 16 h to achieve a homogenous mixture. The AuNP solution was prepared by the reduction of $HAuCl_4$ with trisodium citrate, according to the following literature [24]. Next, MWCNT/Chit-IL solution was added dropwise in the AuNP solution under vigorous agitation until a homogenous black color appears, confirming the formation of MWCNT/Chit-IL/AuNPs nanocomposites. After ultrasonication for an additional 12 h, the black precipitate was isolated via centrifugation at 8500 rpm for 1 h. Finally, the collected precipitates were washed three times with distilled water, dried under a vacuum at 60 °C overnight, and suspended in 1% acetic acid until further use.

Preparation and characterization of modified electrode

First, 6 µl of MWCNT/Chit-IL/AuNPs nanocomposite solution was added dropwise on the screen-printed carbon electrode (SPCE) surface and dried completely. Then, the modified electrode was rinsed thoroughly with 1x phosphate buffered saline (PBS). The dual modified capture probe (3′-end thiol and 5′-end biotins; 1 µM) was prepared by treating with 10 mM TCEP in 0.05 M Tris–HCl containing 0.1 M KCl buffer (pH: 7.2) for 1 h to reduce disulfide bonds. Next, 10 µl of the capture probe was incubated on the MWCNT/Chit-IL/AuNPs/SPCE overnight in a humidified chamber for the formation of Au–S bonds. After washing the electrode with 1x PBS to remove the weakly adsorbed capture probes, 10 µl of 1 mM MCH solution was dropped on the modified electrode surface and incubated for 45 min. Finally, the modified electrode was thoroughly rinsed with 1x PBS, before being used to detect the *KRAS* G12D mutation.

The modified electrode surfaces were analyzed using a field emission scanning electron microscope (FE-SEM; SU8010, Hitachi, Tokyo, Japan), cyclic voltammetry (CV), and electrochemical impedance spectroscopy (EIS) measurements in 10 mM $[Fe(CN)_6]^{3-/4-}$ containing 0.1 M KCl.

Verification of T7EI-mediated cleavage reactions using polyacrylamide gel electrophoresis (PAGE) analysis

To verify the T7EI-mediated cleavage reactions on mutant targets, we rationally designed single-base mismatches (A-C, A-G, and A-A) between the capture probe and target DNA (Online Resource 1). Then, 0.2 μM of the capture probe (A) and target DNA (T, C, G, and A) were hybridized as follows: 95 °C for 5 min; 85 °C for 10 s (− 2 °C/s); 25 °C for 10 s (− 0.1 °C/s). Next, they were cooled at 4 °C for 10 min and then treated with T7EI (2 U/μl) at 37 °C for 1 h. The resulting DNA products were analyzed in 20% native polyacrylamide gel. The gel was pre-run at 200 V for 10 min, and then loaded with DNA products in 1x gel loading dye, and electrophoresis was run at a constant voltage of 160 V for 60 min. Finally, the gel was stained in GreenStar™ Nucleic Acid Staining solution (Bioneer, Daejeon, Korea) for 15 min and then imaged using the ChemiDoc Imaging System (Bio-rad Laboratories, Korea).

Cell culture

Three human colon cancer cell lines (HT29, LS174T, and COLO-205) and two human breast cancer cell lines (MDA-MB-231 and MCF-7) were purchased from the Korean Cell Line Bank and cultured in DMEM and RPMI 1640. Each medium was supplemented with 10% FBS, 100 U/ml penicillin, and 100 μg/ml streptomycin (WELGENE Inc. Gyeongsangbuk-do, Korea). Cells were incubated at 37 °C in a humidified atmosphere of 5% CO_2. Genomic DNA (gDNA) was extracted from cancer cells using a Total DNA Extraction S & V Kit (Bionics Co., Ltd. Daejeon, Korea) and gDNA concentrations were evaluated using a SpectraMax iD5 Microplate Reader (Molecular Devices, Sunnyvale, CA, USA).

Asymmetric PCR amplification

Asymmetric PCR was performed under the following conditions: the initial denaturation at 95 °C for 3 min, followed by 25 cycles of 95 °C for 30 s, 60 °C for 20 s, and 72 °C for 30 s, and then a final extension at 72 °C for 5 min. The amplification was performed in 20 μl of PCR solution containing 50 ng/μl of gDNA, 1.25 U of nPfu-Forte polymerase, 1x nPfu-Forte reaction buffer, and 0.2 mM of dNTPs. A pair of PCR primers at 10:1 ratio (2.5 μM reverse primer:0.25 μM forward primer) was employed to generate the single-stranded DNA (ssDNA) product. The asymmetric PCR products were confirmed via agarose gel electrophoresis.

Electrochemical assay procedure

For DNA hybridization between target DNA and the capture probe on the modified electrode surface, 10 μl of wild (T) or mutant (C) type target DNA in 0.05 M Tris–HCl (pH 7.4) containing 0.1 M KCl was dropped onto the capture probe immobilized on the modified electrode (MWCNT/Chit-IL/AuNPs), followed by incubation for 45 min at room temperature. After washing the electrode surface with 1x PBS to remove the unbound DNA oligonucleotides, 10 μl of T7EI (2 U/μl) was added and incubated at 37 °C for 2 h. Next, the electrode surface was washed with 1x PBS and incubated with 20 μl of SA-HRP polymer (0.01 mg/ml) for 20 min at room temperature to form the biotin-SA-HRP complex, which catalyzes the oxidation reaction of TMB in the presence of H_2O_2. After rinsing the electrode surface, 100 μl of TMB (2 mM) containing H_2O_2 (1 mM) was applied onto the electrode surface for 5 min. Differential pulse voltammetry (DPV) analyses were performed in 20 mM HEPES buffer (pH 6.5; 50 mM KCl and 200 mM NaCl) using potential scanning from 0.1 to 0.6 V with a pulse amplitude of 25 mV.

Results and discussion

Principle of the proposed electrochemical strategy

An overview of the simple electrochemical biosensor for mutation detection by enzymatic cleavage is illustrated in Scheme 1. First, to increase the effective surface area and electrical conductivity, we modified the SPCE with a nanocomposite mixture of MWCNT/Chit-IL/AuNPs, and the dual modified capture probe (3′-end thiol and 5′-end biotin) that can recognize the specific target DNA was immobilized on the modified electrode surface (MWCNT/Chit-IL/AuNPs) through the formation of Au–S bonds. Then, target DNA samples (wild-type or mutant-type) were applied on the modified electrode surface to hybridize with the capture probe. Next, T7EI was used to selectively cleave the mutation site on the dsDNA, as T7EI acts on the mismatch (A-C) formed in the mutant type of target DNA but not on the perfectly matched dsDNA (A-T) of the wild type. As a result, the biotin at 5′-ends of the capture probe hybridized with mutant target samples are removed from the electrode surface, while the capture probes hybridized with wild type target samples remain intact. To get the amplified electrochemical signal, SA-HRP conjugate was applied on the electrode surface to form the biotin-SA-HRP complex, which catalyzes the oxidation reaction of TMB in the presence of H_2O_2. Thus, in the presence of the wild target, an amplified electrochemical signal is produced, but in the presence of the mutant target, a negligible electrochemical signal is generated.

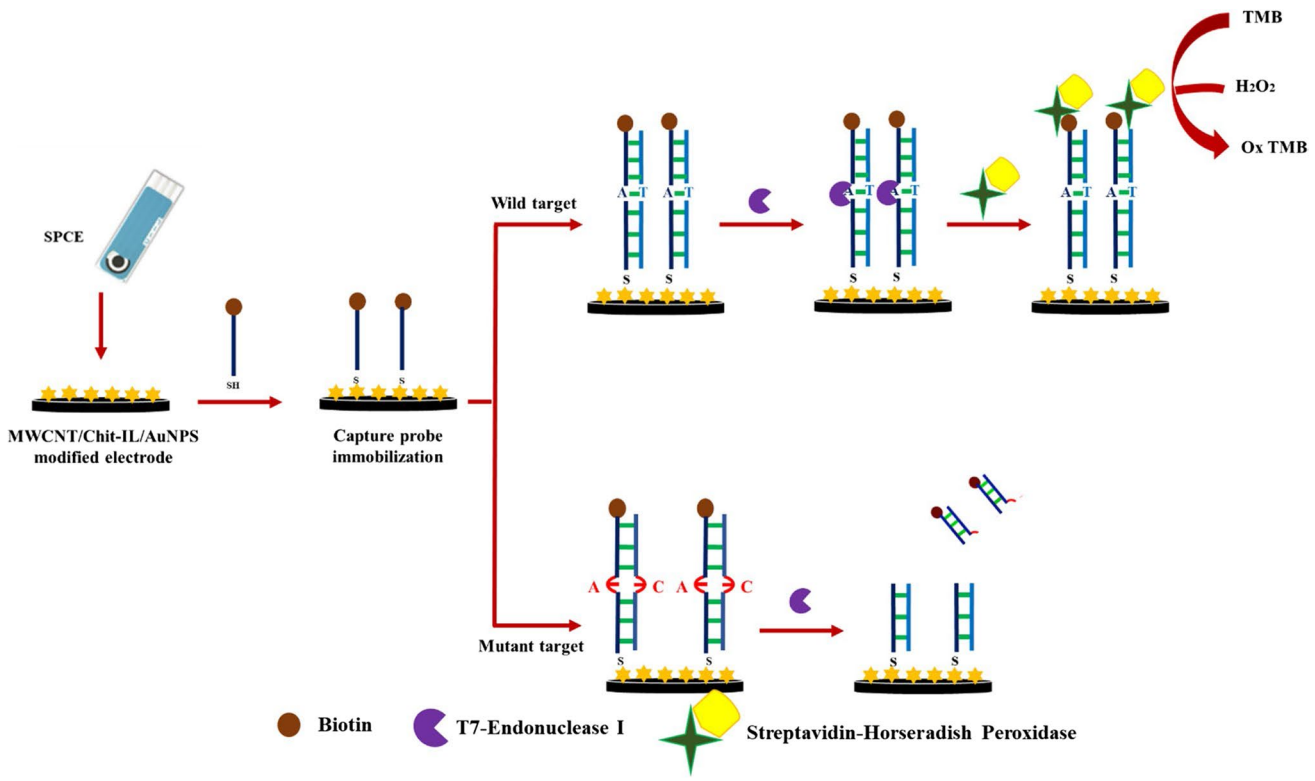

Scheme 1 Schematic illustration of the proposed electrochemical biosensor for mutation detection using T7-Endonuclease I

Characterization of modified sensing interface

Figure 1A presents the morphological images of bare (a), MWCNT/Chit-IL (b), and MWCNT/Chit-IL/AuNP electrodes (c), respectively. Figure 1A(b) indicates the formation of a homogenous and spaghetti-like porous interface of MWCNT/Chit-IL nanocomposite with a high specific surface area on the electrode surface, confirming that functionalized MWCNT was uniformly mixed with chitosan and ionic liquid. In addition, the formation of MWCNT/Chit-IL/AuNPs was demonstrated by the appearance of bright spot on the surface of MWCNTs (Fig. 1A(c) and Online Resource 2), which is attributed to the fact that the AuNPs interact with the free amino groups of both MWCNT and chitosan [25].

Figure 1B shows that the bare electrode (a) displayed a good pair of well-defined redox peaks, whereas in the case of MWCNT/Chit-IL-modified electrode (b), the redox peak current of $[Fe(CN)_6]^{3-/4-}$ was higher than that of the bare one due to the increase in surface area and electron transfer. Importantly, modification with MWCNT/Chit-IL/AuNPs generated the highest current signal (c), indicating the successful modification of the electrode with a large specific surface area and excellent electrical conductivity. The EIS results were also consistent with the CV results. As illustrated in Fig. 1C, the Nyquist plot of modified electrodes showed that the electron transfer resistance (R_{ct}) decreased dramatically when the bare electrode (a) was modified with MWCNT/Chit-IL/AuNPs (c), implying that the modified sensing interface increased the electron transfer rate between the electrode and the $[Fe(CN)_6]^{3-/4-}$ electroactive couple. Furthermore, when the dual modified capture probe (3′-end thiol and 5′-end biotin) was immobilized onto the MWCNT/Chit-IL/AuNP-modified electrode, the redox peak current of $[Fe\ (CN)_6]^{3-/4-}$ was reduced (Fig. 1B(d)) and the R_{ct} was increased (Fig. 1C(d); inset), thereby confirming the successful immobilization of capture probe on the surface of the modified electrode. In addition, the electroactive surface area (A) of MWCNT/Chit-IL and MWCNT/Chit-IL/AuNP-modified electrode was determined according to the Randles-Sevick equation [26].

$$Ip = 2.65 \times 10^5 n^{3/2} A D^{1/2} C v^{1/2}$$

where Ip is the peak current, n is the transferring electron number, A is the electroactive area (cm^2), D is the diffusion coefficient, C is the concentration of the substrate, and v is the scan rate. The diffusion coefficient of redox probe is 7.6×10^{-6} cm^2 s^{-1} [27]. In Online Resource 3A and B, the current density, J ($\mu A \cdot cm^{-2}$) of modified electrodes was proportional to the square root of

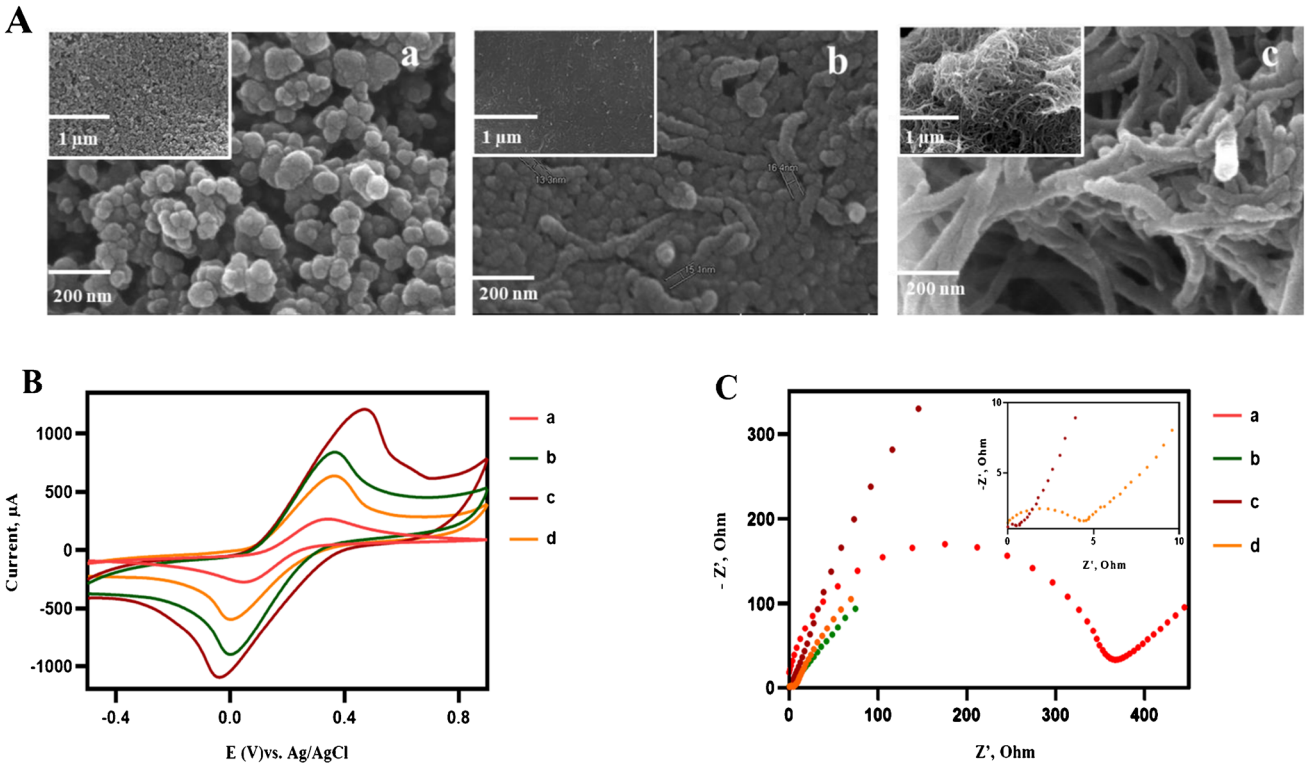

Fig. 1 Characterization of sensing interface. **A** FE-SEM images of (a) bare SPCE, (b) MWCNT/Chit-IL/SPCE, and (c) MWCNT/Chit-IL/AuNPs/SPCE. The scale bars for the high and low magnification (inset) views are 200 nm and 1 µm, respectively. **B** Cyclic voltammetry (CV) and **C** electrochemical impedance spectroscopy (EIS) of (a) bare SPCE, (b) MWCNT/Chit-IL/SPCE, (c) MWCNT/Chit-IL/AuNPs/SPCE, and (d) Dual modified capture probe on MWCNT/Chit-IL/AuNPs/SPCE. CV curves were recorded at a scan rate of 100 mV/s, and EIS data were collected within the frequency range of 10,000 to 0.1 Hz

scan rate. The calculated surface area for each electrode is summarized in Table 1. These results clearly show the significant improvement (*ca.* 220%) compared to bare screen-printed carbon electrode, indicating that the developed materials can be used as the versatile platform for the sensitive electrochemical assay by increasing the electrode surface area and electrochemical signal. Moreover, the stability of the proposed biosensor was high, as evidenced by the results in Online Resource 4.

Table 1 The electroactive surface area of bare screen-printed carbon electrode (SPCE), MWCNT/Chit-IL-modified, and MWCNT/Chit-IL/AuNP-modified electrode

Electrode	Electroactive surface area, A (cm^2)
Bare SPCE	0.11*
MWCNT/Chit-IL	0.16
MWCNT/Chit-IL/AuNPs	0.24

*Metrohm; Autolab SPCE; DRP-C11L

Investigation of T7EI-catalyzed cleavage reactions and detection feasibility

Although T7EI is known to recognize and cleave non-perfectly matched dsDNA, it is important to determine the cleavage efficiency of all single base pair mismatches in heteroduplex DNA [28, 29]. As shown in Fig. 2A, the A-C mismatch was the most effectively recognized and completely cleaved by T7EI. On the other hand, the cleavage efficiencies of other mismatches (A-G and A-A) were not as effective as that of the A-C mismatch. This result proves that T7EI can recognize single-base mismatch sites in heteroduplex DNA, where at least one of the mismatched bases contain cytosine [30].

To demonstrate the feasibility of the proposed electrochemical detection strategy, reactions were performed under different conditions and the resulting DPV signals were measured. As shown in Fig. 2B and Online Resource 5, when there is no target DNA, a high electrochemical signal was observed regardless of the presence of T7EI (curves a and b, respectively) because the biotin on the capture probe was intact, and thus, the biotin-SA-HRP complex

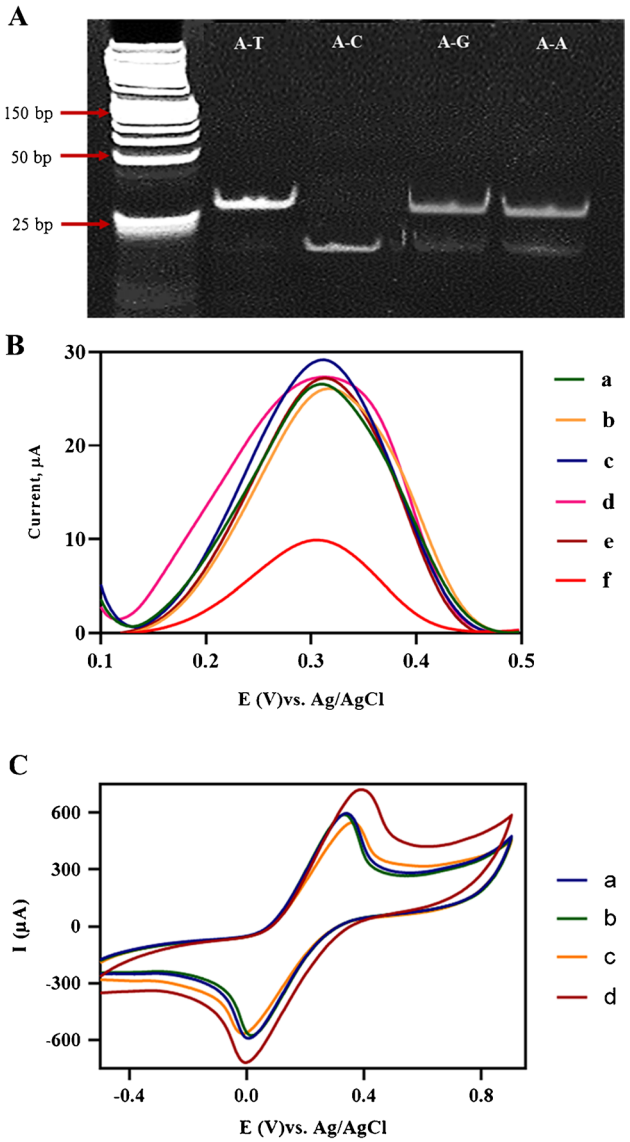

Fig. 2 Investigation of T7-Endonuclease I (T7EI)-catalyzed reactions and detection feasibility. **A** Gel electrophoresis of heteroduplex DNA treated with T7EI. Lane 1: A-T base pair (perfectly matched); Lane 2: A-C mismatch base pair; Lane 3: A-G mismatch base pair; Lane 4: A-A mismatch base pair. **B** Differential pulse voltammetry (DPV) signals under different detection conditions (a) capture probe without T7EI, (b) capture probe with T7EI, (c) capture probe/wild target without T7EI, (d) capture probe/wild target with T7EI, (e) capture probe/mutant target without T7EI, and (f) capture probe/mutant target with T7EI. **C** Electrochemical interfacial properties of the proposed biosensor (a) capture probe/wild target/without T7EI treatment, (b) capture probe/wild target/with T7EI treatment, (c) capture probe/mutant target/without T7EI treatment, and (d) capture probe/mutant target/with T7EI treatment. Cyclic voltammetry was performed in 10 mM $[Fe(CN)_6]^{3-/4-}$ and 0.1 KCl solution at a scan rate of 100 mV/s

was formed, allowing TMB to be oxidized. When the wild target was hybridized with capture probe, a high electrochemical signal was also generated in both the absence and presence of T7EI (curves c and d, respectively), which is comparable to the signal without target DNA. In contrast, probing the mutant target resulted in a different DPV signal in the presence of T7EI. Specifically, in the absence of T7EI, a high electrochemical signal was generated (curve e); however, upon T7EI treatment, the DPV signal significantly decreased (curve f) due to the removal of biotin moieties. These results validated the applicability of the prepared biosensor to the detection of the mutant target. In addition, the interfacial properties of the fabricated biosensor were also examined via CV analysis. As shown in Fig. 2C, the hybridization of target DNA (wild or mutant) with capture probe on the modified electrode surface produced similar redox currents of $[Fe(CN)_6]^{3-/4-}$ (curves a and c), which was likely due to the electrostatic repulsion between the negatively charged $[Fe(CN)_6]^{3-/4-}$ ions in the solution and the negatively charged phosphate backbone of the DNA on the surface of the electrode. To evaluate the cleavage activity via T7EI, the hybridized DNA was treated with T7EI. As expected, the mismatch site in the mutant target was recognized and cleaved by the T7EI, and the dsDNA became shorter, resulting in the increased redox current of $[Fe(CN)_6]^{3-/4-}$ (curve d). On the contrary, T7EI treatment did not affect the matched dsDNA (wild-type target) (curve b) showing a redox current peak similar to the ones without T7EI treatment (curve a and c). These CV results support the detection feasibility of our developed biosensor.

Sensitivity and selectivity of the proposed biosensor

To obtain the best performance of the proposed electrochemical biosensor, we optimized the reaction conditions required for the efficient analysis of target mutations by examining the current responses. In a series of experiments, we varied the composite percentage of MWCNT/Chit-IL and AuNPs, the hybridization time between capture probe and target, and T7EI concentration and incubation time. The results show that the ideal conditions for detection of the mutant gene are as follows: 13% and 87% (v/v) of MWCNT/Chit-IL and AuNP solution to prepare the nanocomposite, 45 min of hybridization time, 2 h of T7EI reaction time, and 2 U/μL concentration of T7EI on the electrode surface (Online Resource 6 A–E).

Under the optimized conditions, the detection sensitivity of the assaying system was determined by measuring the DPV signals with various mutant target concentrations ranging from 1 μM to 100 fM (Fig. 3A a–h; i: blank). As shown in Fig. 3A, the TMB oxidation peak currents increased with the decreasing concentration of the mutant target, demonstrating that the cleavage efficiency of T7EI is dependent on the amount of mutant target. In Fig. 3B, the plot of DPV current vs. the logarithm of mutant target concentrations

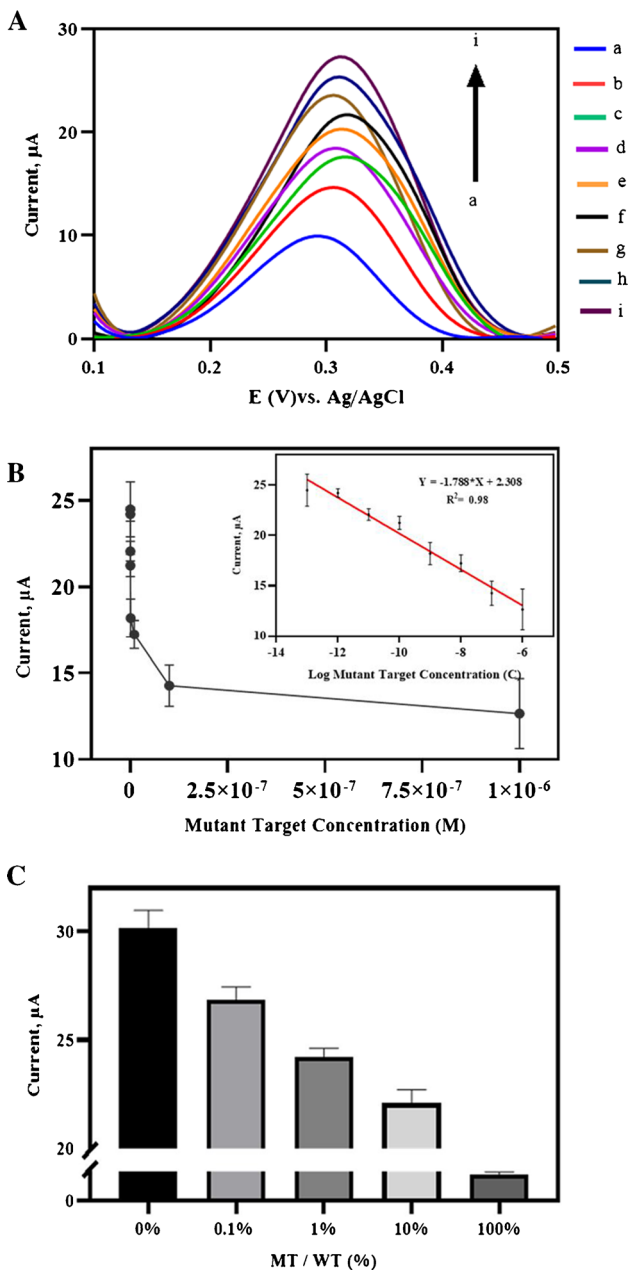

Fig. 3 Detection sensitivity and selectivity of the developed biosensor. **A** Differential pulse voltammetry (DPV) signals in the presence of different concentrations of mutant target DNA (a–i: 1 μM, 100 nM, 10 nM, 1 nM, 100 pM, 10 pM, 1 pM, 100 fM, and blank, respectively). **B** The calibration plot of the DPV peak current versus concentrations of the mutant target DNA (from 1×10^{-13} M to 1×10^{-6} M). Inset shows the linear relationship of the DPV peak current versus log concentrations of the mutant target DNA (from log 1×10^{-13} (−13 M) to log 1×10^{-6} M (−6 M)). The maximum DPV current was obtained at 0.3 V by measuring from 0.1 to 0.6 V with a pulse amplitude of 25 mV. **C** Comparison of current response in the mixtures of mutant/wild targets with different molar ratios (mutant target: 0, 0.1%, 1%, 10%, and 100%; wild target: fixed at 100 pM). Error bars were derived from three separate assays

showed a broad linear range with a coefficient correlation of 0.98. The limit of detection (*LOD*) is calculated to be 11.89 fM, based on definition of $LOD = 3\sigma/m$ (where σ is the standard deviation of the blank signal, and m is the slope of the linear calibration plot), which is comparable or superior to the *LOD* of previous detection systems (Online Resource 7).

To evaluate the selectivity of this biosensor for mutation detection, we evaluated whether the biosensor could detect mutant targets in the presence of large amounts of wild targets. The mixtures of mutant/wild targets with different molar ratios (0.1%, 1%, 10%, and 100%) were analyzed using the proposed biosensor, wherein the concentration of wild targets was fixed at 100 pM. Figure 3C shows that the DPV signals decreased with the increasing molar ratio of mutant target DNA. It is noticeable that 0.1% of the mutant DNA could be discriminated from the wild target DNA (p value = 0.0044, two-tailed t test), which is comparable or superior to other methods [31, 32]. These results confirm that the proposed method has an excellent capability to detect even a low-abundance mutation in a large background of wild-type targets, implying its potential for clinical application. These results show that our developed biosensor has potential application for the detection of mutated genes in cancer cells. Moreover, the proposed biosensor is not only applicable for the specific mutation detection but also for the detection of other target molecules by employing the specific receptors such as antibody or aptamers. Since there are many antibodies or aptamers specific to drugs, herbicides, pesticides, etc., [33, 34] this proposed biosensor can serve as a versatile platform for the detection of various target species.

Mutation detection in cancer cells

To assess the applicability of the prepared biosensor for mutation detection, experiments were carried out in cancer cell lines. We selected the colorectal cancer cell lines COLO-205 and HT29, and breast cancer cell lines MDA-MB-231 and MCF-7, as *KRAS* G12D wild-type cell lines, while LS174T (colorectal cancer) was selected as the *KRAS* G12D mutant cell line. Genomic DNA from each cell line was first extracted and amplified by asymmetric PCR to generate 112 bp single-stranded DNA targets (Online Resource 8), which could hybridize with the capture probe on the modified electrode. Next, amplicons from different cell lines were applied on the developed biosensors. As shown in Fig. 4, the diminished DPV signal was only observed in the mutant-type cell line LS174T, while other four wild-type cell lines generated high current signals. These results show that our developed biosensor has potential application for the detection of mutated genes in cancer cells.

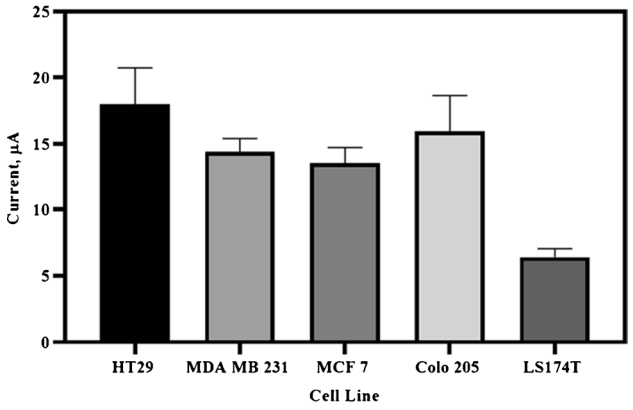

Fig. 4 Mutation detection of genomic DNA from different cell lines. (a) HT29, (b) MDA-MB-231, (c) MCF-7, (d) COLO-205, and (e) LS174T. Error bars were derived from three separate assays

Conclusion

We developed a simple electrochemical biosensor for the detection *KRAS* mutants by T7 Endonuclease I. The biosensor developed in this study provides an easy, time-saving, robust, sensitive, and selective approach for mutation detection. It has a high potential for application to detect other cancer-related mutations, enabling early diagnosis of cancer and more versatile use in biomedical research. Moreover, the proposed assay can be applied for the detection of other genetic biomarkers by designing the artificial mismatch to be formed with the capture probe, which can be cleaved by T7EI. We believe that this platform can be used for the sensitive and specific detection of various genetic biomarkers.

Supplementary Information The online version contains supplementary material available at https://doi.org/10.1007/s00604-021-05089-1.

Author contribution Pinky Chowdhury: conceptualization, methodology, validation, formal analysis, investigation, writing—original draft. Byung Seok Cha: methodology, formal analysis, review. Seokjoon Kim: methodology, formal analysis. Eun Sung Lee: methodology, formal analysis. Taehwi Yoon: formal analysis. Jisu Woo: formal analysis. Ki Soo Park: writing—review and editing, funding acquisition, resources, supervision.

Funding This work was supported by a grant from the National Research Foundation of Korea (NRF), funded by the Korea government (Ministry of Science and ICT) (No. NRF-2020R1C1C1012275), Korea Institute of Energy Technology Evaluation and Planning (KETEP) and the Ministry of Trade, Industry and Energy (MOTIE, 20194010201900), and by Konkuk University Researcher Fund in 2021.

Declarations

Competing interests The authors declare no competing interests.

References

1. Liu P, Wang Y, Li X (2019) Targeting the untargetable KRAS in cancer therapy. Acta Pharm Sin B 9(5):871–879. https://doi.org/10.1016/j.apsb.2019.03.002
2. Porru M, Pompili L, Caruso C, Biroccio A, Leonetti C (2018) Targeting KRAS in metastatic colorectal cancer: current strategies and emerging opportunities. J Exp Clin Cancer Res 37(1):57. https://doi.org/10.1186/s13046-018-0719-1
3. Walther A, Johnstone E, Swanton C, Midgley R, Tomlinson I, Kerr D (2009) Genetic prognostic and predictive markers in colorectal cancer. Nat Rev Cancer 9(7):489–499. https://doi.org/10.1038/nrc2645
4. Chiu HM, Chang LC, Hsu WF, Chou CK, Wu MS (2015) Noninvasive screening for colorectal cancer in Asia. Best Pract Res Clin Gastroenterol 29(6):953–965. https://doi.org/10.1016/j.bpg.2015.09.015
5. Chung EJ, Yeom SS, Bonhan K, Tae YL, Jeong HL, Yong S, Lim SB (2017) Rapid and accurate detection of KRAS mutations in colorectal cancers using the isothermal-based optical sensor for companion diagnostics. Oncotarget 8(48):83860–83871
6. Li Y, Monzo M, Moreno I, Martinez-Rodenas F, Hernandez R, Castellano JJ, Canals J, Han B, Munoz C, Navarro A (2020) KRAS mutations by digital PCR in circulating tumor cells isolated from the mesenteric vein are associated with residual disease and overall survival in resected colorectal cancer patients. Int J Colorectal Dis 35(5):805–813. https://doi.org/10.1007/s00384-020-03538-6
7. Cha BC, Park KS, Park JS (2020) Signature mRNA markers in extracellular vesicles for the accurate diagnosis of colorectal cancer. J Biol Eng 14(1). https://doi.org/10.1186/s13036-020-0225-9
8. Hashkavayi AB, Cha BS, Hwang SH, Kim J, Park KS (2021) Highly sensitive electrochemical detection of circulating EpCAM-positive tumor cells using a dual signal amplification strategy. Sensors Actuators B Chem 343130087. https://doi.org/10.1016/j.snb.2021.130087
9. Malhotra P, Anwar M, Nanda N, Kochhar R, Wig JD, Vaiphei K, Mahmood S (2013) Alterations in K-ras, APC and p53-multiple genetic pathway in colorectal cancer among Indians. Tumour Biol 34(3):1901–1911. https://doi.org/10.1007/s13277-013-0734-y
10. Lang AH, Drexel H, Geller-Rhomberg S, Stark N, Winder T, Geiger K, Muendlein A (2011) Optimized allele-specific real-time PCR assays for the detection of common mutations in KRAS and BRAF. J Mol Diagn 13(1):23–28. https://doi.org/10.1016/j.jmoldx.2010.11.007
11. Tommy N, Mostofa R, Lena F (2000) Ulf dF, Ralf M, Pal N (2000) Direct analysis of single-nucleotide polymorphism on double-stranded DNA by pyrosequencing. Biotechnol Appl Biochem 31:107–112. https://doi.org/10.1042/BA19990104
12. Kam Y, Rubinstein A, Nissan A, Halle D, Yavin E (2012) Detection of endogenous K-ras mRNA in living cells at a single base resolution by a PNA molecular beacon. Mol Pharm 9(3):685–693. https://doi.org/10.1021/mp200505k
13. Okumura A, Sato Y, Kyo M, Kawaguchi H (2005) Point mutation detection with the sandwich method employing hydrogel nanospheres by the surface plasmon resonance imaging technique. Anal Biochem 339(2):328–337. https://doi.org/10.1016/j.ab.2005.01.017
14. Zhang Y, Wang L, Luo F, Qiu B, Guo L, Weng Z, Lin Z, Chen G (2017) An electrochemiluminescence biosensor for Kras mutations based on locked nucleic acid functionalized DNA walkers and hyperbranched rolling circle amplification. Chem Commun (Camb) 53(20):2910–2913. https://doi.org/10.1039/c7cc00009j

15. Xiao Q, Feng J, Li J, Liu Y, Wang D, Huang S (2019) A ratiometric electrochemical biosensor for ultrasensitive and highly selective detection of the K-ras gene via exonuclease III-assisted target recycling and rolling circle amplification strategies. Anal Methods 11(32):4146–4156. https://doi.org/10.1039/c9ay01007f
16. He Y, Cheng L, Yang Y, Chen P, Qiu B, Guo L, Wang Y, Lin Z, Hong G (2020) Label-free homogeneous electrochemical biosensor for HPV DNA based on entropy-driven target recycling and hyperbranched rolling circle amplification. Sens Actuators B: Chem 320. https://doi.org/10.1016/j.snb.2020.128407
17. Yang X, Lv J, Yang Z, Yuan R, Chai Y (2017) A sensitive electrochemical aptasensor for thrombin detection based on electroactive co-based metal-organic frameworks with target-triggering NESA strategy. Anal Chem 89(21):11636–11640. https://doi.org/10.1021/acs.analchem.7b03056
18. Chang Y, Zhuo Y, Chai Y, Yuan R (2017) Host-guest recognition-assisted electrochemical release: its reusable sensing application based on DNA cross configuration-fueled target cycling and strand displacement reaction amplification. Anal Chem 89(16):8266–8272. https://doi.org/10.1021/acs.analchem.7b01272
19. Zhao C, Gao F, Weng S, Liu Q, Lin L, Lin X (2016) An electrochemical sensor based on DNA polymerase and HRP-SiO2 nanoparticles for the ultrasensitive detection of K-ras gene point mutation. RSC Adv 6(11):8669–8676. https://doi.org/10.1039/c5ra24737c
20. Fang X, Bai L, Han X, Wang J, Shi A, Zhang Y (2014) Ultrasensitive biosensor for K-ras gene detection using enzyme capped gold nanoparticles conjugates for signal amplification. Anal Biochem 460:47–53. https://doi.org/10.1016/j.ab.2014.05.019
21. Sun N, Guo Q, Li X, Chen J, Liu X, Wong K-Y, Fang Z (2018) An isothermal single base extension based lateral flow biosensor and electrochemical assay for gene point mutation detection. Anal Methods 10(24):2863–2868. https://doi.org/10.1039/c8ay00746b
22. Gosselin D, Gougis M, Baque M, Navarro FP, Belgacem MN, Chaussy D, Bourdat AG, Mailley P, Berthier J (2017) Screen-printed polyaniline-based electrodes for the real-time monitoring of loop-mediated isothermal amplification reactions. Anal Chem 89(19):10124–10128. https://doi.org/10.1021/acs.analchem.7b02394
23. Hashkavayi AB, Raoof JB, Ojani R (2018) Preparation of epirubicin aptasensor using curcumin as hybridization indicator: competitive binding assay between complementary strand of aptamer and epirubicin. Electroanalysis 30(2):378–385. https://doi.org/10.1002/elan.201700645
24. Zhang X, Huang C, Jiang Y, Shen J, Geng P, Zhang W, Huang Q (2016) An electrochemical glycan biosensor based on a thionine-bridged multiwalled carbon nanotube/gold nanoparticle composite-modified electrode. RSC Adv 6(114):112981–112987. https://doi.org/10.1039/c6ra23710j
25. Leszek AD, Mirka P, Andrzej K, Barbara L (2009) Synthesis and characterization of carbon nanotubes decorated with gold nanoparticles. Acta Physica Polonica Series a. https://doi.org/10.12693/APhysPolA.118.483
26. Bai L, Yuan R, Chai Y, Yuan Y, Wang Y, Xie S (2012) Direct electrochemistry and electrocatalysis of a glucose oxidase-functionalized bioconjugate as a trace label for ultrasensitive detection of thrombin. Chem Commun (Camb) 48(89):10972–10974. https://doi.org/10.1039/c2cc35295h
27. Qin X, Guo W, Yu H, Zhao J, Pei M (2015) A novel electrochemical aptasensor based on MWCNTs–BMIMPF6 and amino functionalized graphene nanocomposite films for determination of kanamycin. Anal Methods 7(13):5419–5427. https://doi.org/10.1039/c5ay00713e
28. Murugesan SN, Connahs H, Matsuoka Y (2021) Gupta Md, Huq M, Gowri V, Monroe S, Deem KD, Werner T, Tomoyasu Y. Monteiro A. https://doi.org/10.1101/2021.03.01.429915
29. Sentmanat MF, Peters ST, Florian CP, Connelly JP, Pruett-Miller SM (2018) A survey of validation strategies for CRISPR-Cas9 editing. Sci Rep 8(1):888. https://doi.org/10.1038/s41598-018-19441-8
30. Chudi G, Sanjay K, Rebecca K, Amy E (2004) Changing the enzymatic activity of T7 endonuclease by mutations at the â-Bridge Site: alteration of substrate specificity profile and metal ion requirements by mutation distant from the catalytic domain. Biochemistry 43(14). https://doi.org/10.1021/bi036033j.
31. Nahm FS (2017) What the P values really tell us. Korean J Pain 30(4):241–242. https://doi.org/10.3344/kjp.2017.30.4.241
32. Griffiths P, Needleman J (2019) Statistical significance testing and p-values: defending the indefensible? A discussion paper and position statement. Int J Nurs Stud 99:103384. https://doi.org/10.1016/j.ijnurstu.2019.07.001
33. Abnous K, Danesh NM, Alibolandi M, Ramezani M, Taghdisi SM (2017) Amperometric aptasensor for ochratoxin A based on the use of a gold electrode modified with aptamer, complementary DNA, SWCNTs and the redox marker Methylene Blue. Microchim Acta 184(4):1151–1159. https://doi.org/10.1007/s00604-017-2113-7
34. Han K, Liu T, Wang Y, Miao P (2016) Electrochemical aptasensors for detection of small molecules, macromolecules, and cells. Rev Anal Chem 35(4):201–211. https://doi.org/10.1515/revac-2016-0009